

Ages of globular clusters: a new approach

Raul Jimenez,^{1,2} Peter Thejll,² Uffe G. Jørgensen,² James MacDonald³
and Bernard Pagel¹

¹*NORDITA, Blegdamsvej 17, DK-2100 Copenhagen, Denmark*

²*Niels Bohr Institute, Blegdamsvej 17, DK-2100 Copenhagen, Denmark*

³*Dept. of Physics and Astronomy, University of Delaware, Newark, DE 19716, USA*

ABSTRACT

We have applied a new method to analyze the horizontal branch (HB) morphology in relation to the distribution of stars near the red giant branch (RGB) tip for the globular clusters M22, M5, M68, M107, M72, M92, M3 and 47 Tuc. This new method permits determination of the cluster ages to greater accuracy than conventional isochrone fitting. Using the method in conjunction with our new high-quality photometric data for RGB and HB stars in the first five of these clusters, we discuss the origins of the spread in color on the HB and its relation to the ‘second parameter’ problem. The oldest clusters in our sample are found to have relatively low ages (13.5 ± 2 Gyr). A 1σ uncertainty in each of the parameters of mass and helium content combined with the effects of helium diffusion gives a lower limit for the age of the oldest clusters of 9.7 Gyr.

Key words: stars: mass-loss – stars: horizontal branch – stars:evolution – globular clusters: general – cosmology: age of the universe

1 INTRODUCTION

Globular clusters (GC) probably contain the oldest identifiable stars and are therefore suitable for work on determining lower limits to the age of the Universe. Re-assessment of globular cluster ages is timely in view of recent ground-based and HST observations of Cepheid variables in Virgo cluster galaxies (Pierce et al 1994; Freedman et al 1994) which give a Hubble constant of 87 ± 7 and 80 ± 17 km s⁻¹ Mpc⁻¹ respectively. In the simplest inflationary Universe ($\Omega = 1$, $\Lambda = 0$) this corresponds to ages of 7.7 ± 0.6 and 8.7 ± 1.8 Gyr, respectively, with a 50% increase if $\Omega = 0$. These age estimates are much lower than previously thought and in particular are lower than many estimates of the ages of the oldest globular clusters (Salaris, Chieffi and Straniero 1993, McClure et al. 1987). The era of CCD photometry has brought an impressive increase in the accuracy of the data available for GC analysis at the same time as rapid improvements in theoretical work on GCs. Deficiencies in the input physics combined with the uncertainties in cluster distances and interstellar reddening have made it difficult to determine globular cluster ages with an accuracy better than about 25%.

The questions that we want to answer in this paper are:

- i) What is the origin of the spread in effective temperature along the HB?
- ii) How is the morphology of the HB related to the morphology of the RGB tip?

iii) Is it possible to constrain the mass loss efficiency and the mass of the RGB from the morphology of the HB?

iv) If so what is the age of the GCs and what are the uncertainties involved?

v) How is the ‘second parameter’ related to the origin of the morphology of the HB?

Since the earliest theoretical stellar evolution sequences for low-mass stars, major efforts have been made to calculate globular cluster ages (VandenBerg 1988). The most popular method, isochrone fitting (Sandage 1982, VandenBerg 1983), is to fit the observed GC main-sequence with appropriate main sequence theoretical isochrones. The age of the cluster is gauged from the position of the observed main sequence turnoff relative to the isochrones. The most important ingredient of this method, as we see it, is the necessary assumption of a description of the efficiency of convective energy transport in modelling stellar structure and evolution – often treated by a mixing length theory (e.g. Böhm–Vitense 1958) – and this assumption’s influence on the structure of the star. The ‘mixing length parameter’ (α), which is one of several parameters that determine the convective efficiency (the others are often left at fixed canonical values), is often chosen *a priori*. Usually a value is chosen that is close to the value found in calibrations of solar-type models to the Sun’s observed luminosity, radius and/or temperature (not all observables of the Sun are always used in the calibration, and unfortunately it is not uncommon to find fits in the litera-

ture that have been done using the solar models at a wrong age and/or metallicity – see Jørgensen (1991) for a more complete discussion). Although the Sun may not be similar to other low-mass stars in chemically different systems such as GCs, the assumption is, apparently, that we do at least know the Sun very well; this argument is not often touched upon, see VandenBerg (1983 section V) for one of the few published comments on this problem. The typical error in the age determination for the isochrone fitting method, excluding that due to the mixing-length parameter problem, is about 3 Gyr, and is mainly due to uncertainties in reddening, distance modulus and the position of the turnoff, as has been discussed by Chaboyer (1995).

In order to avoid some of these problems, Iben and Renzini (1984) presented another method to determine GC ages from a calibration of the magnitude difference between the horizontal branch (HB) and the main-sequence turnoff, at the color of the turnoff. The method relies on the fact that the luminosity of the ZAHB is probably not a function of age, while that of the turnoff obviously is. The main disadvantage of this method is that many GCs show either a very blue or a very red HB, and it is difficult to estimate with any certainty the location of the ZAHB at the color of the turnoff. This method also suffers from the difficulty of precisely locating the turnoff. A 0.3 mag. error (VandenBerg 1988) in the observed magnitude difference corresponds to an error of 5 Gyr in the age determination.

A third approach to measure relative ages for star clusters with similar chemical compositions was developed by VandenBerg, Bolte and Stetson (1990). This method uses the fact that the color difference between the turnoff and the base of the giant branch, $\delta(B - V)$, decreases as the cluster age increases. Therefore, aligning all the colour-magnitude diagrams (CMDs) and looking at the positions of the different RGBs will give an age estimate. The obvious limitation of this method is that it only applies to clusters with the same metallicity. Nevertheless, this method introduced an important procedure in the process of understanding GCs: relative morphological arguments. Using relative morphological arguments the authors were able to give much more accurate relative ages than before. Unfortunately the same authors concluded that no relative morphological argument could be used to give an absolute age determination. We will show in this paper how this is not necessarily true and how the power of morphological constraints can lead to an accurate determination of GC ages.

The above three methods have been applied to several globular clusters. The age found for clusters like M92 and M68 ranges from values like 19 Gyr (Salaris, Chieffi and Straniero 1993), with the α -elements (O, Ne, Mg, Si, S, and Ca) enhanced relative to iron, to 14 Gyr (VandenBerg 1988) for [O/Fe] enhanced models with the ratios of the other α -elements to iron kept at the solar value, and a larger distance modulus. Therefore, the difference in the value for the age is quite large (33%). It is also evident that an increasing number of ‘control-parameters’ (like oxygen enhancement, increased helium abundance, etc) affect the results of such work. For instance, Bergbusch & VandenBerg (1992) tested the effects on the age question of adding only oxygen. However, without explicit calculations it is not clear how the non-solar abundance ratios should be handled.

In order to illuminate this central question in cosmology

and stellar evolution we have developed a new method to determine GC ages. The method is based on an accurate determination of the mass of the RGB stars and of α at the RGB, as well as quantitative determination of the mass loss along the RGB, which is constrained by the HB morphology. These theoretical improvements have been complemented with accurate multi-band photometry (UBVR_IJHK) for five GCs that we have gathered during the past year. In addition, we have analyzed data from the literature for three other well studied clusters (M92, M3 and 47 Tuc).

While the mixing length parameter α is but a crude approximation to stellar convection, we can show that its use is consistent and is meaningful in the relatively short-lived RGB stars in clusters, since at this stage of evolution of GC RGB stars the physical conditions of the stars are similar.

Since GCs are observed to have extended HBs one infers that there is variation in the parameter or parameters that determine the colour of HB stars. The ratio of core mass to total stellar mass, (q), is one parameter that influences HB star colour, but metallicity also plays a role. As the stars evolve from the ZAHB, they may move along the HB and thus appear at a colour that is also a function of the time since arrival on the HB. It is well known that, of these factors, q is the most important (Rood 1973). In the ratio q , the core mass for stars recently arrived from the RGB tip (i.e. within a few HB star lifetimes - a few times 10^8 years), is a narrowly constrained number near $0.5 M_{\odot}$ due to the physics of the He core flash in low mass stars. The only variable that is left for producing variations in q , and thus in HB color, is the total mass or, since the core mass is more or less fixed, the mass of the envelope left on top of the core following the RGB evolution. The early work by Rood (1973) made clear the necessity for a spread in the mass to explain the morphology of the HB (Lee, Demarque & Zinn 1994), but there was no attempt to do a quantitative analysis and link its properties with the rest of the HR-diagram. Jørgensen & Thejll (1993) investigated quantitatively which parameters can model the HB consistently with the morphology of the RGB. They concluded that only two possible scenarios could account for the HB morphology: stochastic variations in the mass loss efficiency and/or a delayed helium core flash due, for instance, to rotation. With our new observational material and new theoretical tools, we now conclude that the morphology of the HB can only be explained by stochastic variations in the mass loss efficiency. Also we put strong limits on the variations in the mass loss efficiency by analysing the morphology at the RGB tip.

In this paper we present new observations and theoretical tools that bring clues about three important subjects in GC studies: the physical origin of the spread in temperature on the HB, the ‘second parameter’ problem and the age of the GCs. In sections 2 and 3, we describe the observations and data reductions. In section 4, we describe the theoretical tools used to analyse HB morphology in GCs and red giant branch tip (RGT) morphology. In section 5, we present the analysis of the HB morphology in terms of differential mass loss processes. In section 6, we use the previous tools to analyse the set of GCs and calculate their ages. We finish in section 7 with a critical comparison with previous studies from the literature.

2 OBSERVATIONS AND DATA REDUCTIONS

We obtained UBVRIJK photometry of the GCs M22, M107, M72, M5, and M68 in June 1993 at La Silla (Chile) using the Danish 1.5m telescope and the ESO 2.2m telescope. Here we concentrate on the optical photometry – the IR photometry will be described in a forthcoming paper.

The observations at the Danish 1.5m telescope were taken with a 1024×1024 pixels CCD. Dark, bias and flat frames were taken in order to remove the instrumental signature from the data. The flat field frames were observed both on the sky during twilight and on the dome. The clusters were covered in each filter with one frame, but several frames were taken of the same cluster and the same filter in order to improve the signal-to-noise ratio. Typical exposure times were 60 s to 200 s for the V filter, and about 1800 s for the U filter. For the flat field twilight exposures we used a range of 30 s for the B,V,R and I filters to 200 s for the U filter. Since we were only interested in investigating the giants and HB stars, we did not perform photometry deep enough to reach the main sequence turnoff in most cases.

All data reductions were carried out with utilities in the IRAF package. All science frames were corrected for dark current, bias level and pixel to pixel variations in response to illumination. Standard stars with a wide range in colour, selected from the list of Landolt (1992), were observed through the night at various air masses.

Photometry of cluster stars was reduced using DAOPHOT II (Stetson 1987). The point spread function was determined from 10 bright, isolated stars in each frame. A constant and a linear model for the PSF were used to extract magnitudes; since both methods lead to the same result, a constant PSF was chosen in the reductions. Averaging of the approximately 20 available frames for each filter was performed to obtain the best possible signal.

In order to improve the accuracy of the photometry to the statistical limit and to obtain the best possible results for a morphological analysis, we used an additional algorithm to decrease the errors in the magnitudes. This is based on the idea that while all stars in a single frame may be well calibrated relative to the standards, the standard star fields and the cluster frames were necessarily taken at slightly different times and in different directions on the sky. Small, otherwise undetectable atmospheric disturbances, variations in the atmospheric water content, turbulence, small wings in the PSF, etc., could therefore offset each cluster frame from the others which will result in a larger error than that due to the calibration process itself. We selected in one frame around 100 of the most well behaved stars, i.e. those that are reasonably isolated and far away from the edge of the frame and which show low scatter in the color-magnitude diagram (CMD) – such as a section of the RGB between the top of the sub-giant branch and the HB. Using the coordinates of these stars, we found them in each of the frames for the relevant filter. In each frame, we then calculated the 100-star average of the selected stars and then expressed the magnitudes of all stars in each frame relative to the 100-star average. This step removes small offsets in the photometry since each frame is probably affected uniformly across the field by any thin cirrus or dust. By averaging these frames we can then reduce the statistical errors. It then remains to calibrate these ‘atmospheric disturbance-free’ frames onto

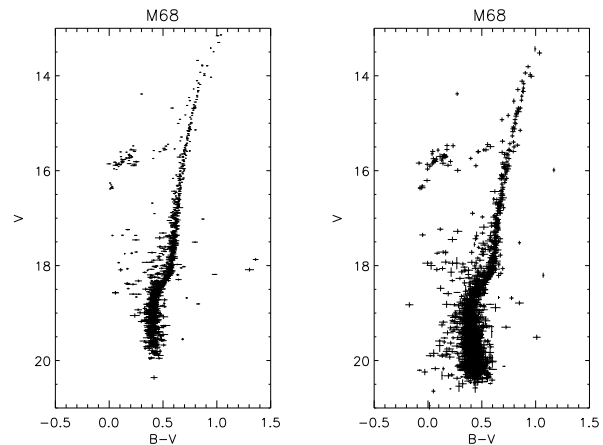


Figure 1. The figure shows the errors in the photometry of the globular cluster M68 using two methods to reduce the data. The panel to the right shows the standard method of averaging, while the panel to the left shows the improvements in photometry due to the additional reduction step we have introduced – see section 2. The brightest stars at $V=12.5^m$ have not been included here owing to overexposure (see McClure et al 1987, where the brightest stars were taken from photographic photometry).

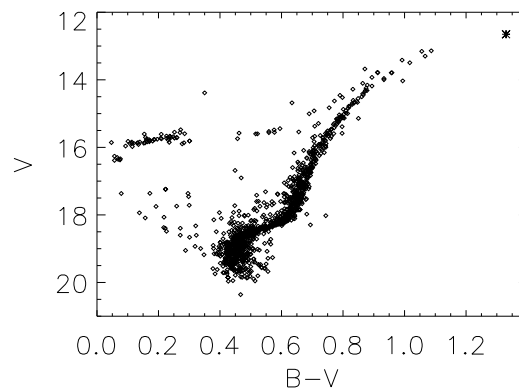


Figure 2. HR-diagram for the globular cluster M68. The size of the symbols is about that of the errors. There is a clear split between the RGB and the AGB. The ‘star’ shows the position of the two reddest stars in the cluster measured photographically by Harris (1975).

the standard star system of photometry. This step is done by shifting the ‘atmospheric disturbance-free’ frames back to the photometric values present in the calibrated and averaged ‘possibly slightly atmospheric disturbed’ frames of the previous paragraph. If the effects of the postulated atmospheric disturbances are normally distributed then the above process will lead to photometry with no worse offsets in magnitudes than those present in the ‘possibly slightly atmospheric disturbed’ frames and with photometric errors on each star substantially lower. As shown in Figure 2 for the cluster M68, the improvement in the photometric errors is quite significant. In Figures 2 to 6 we show the HR-diagrams for the five GCs observed.

To make theoretical predictions, we need to transform

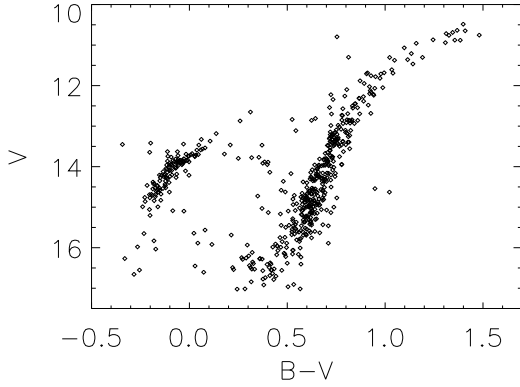


Figure 3. Colour–magnitude diagram for the globular cluster M22. The cluster shows a very blue HB and a broad RGB. The thickness of the RGB is bigger than the photometric errors. In the text we show how this intrinsic broadening of the RGB and AGB can be due to metallicity variations in the GC.

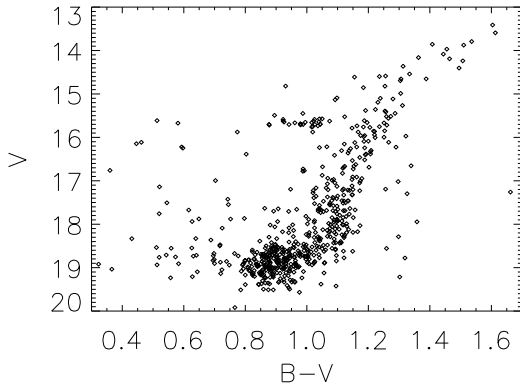


Figure 4. The GC M107 has a very broad RGB. The errors in the photometry are much smaller than the thickness of the RGB – the size of the symbols is approximately that of the errors. It is important to be aware of the field contamination in this cluster.

the observed $(B - V)$ vs. V diagram to the theoretical L vs. T_{eff} diagram. To do this it is necessary to know several parameters, such as the distance modulus $(m - M)_V$, the reddening $E(B - V)$, the metallicity Z , the helium content Y and the theoretical transformation from $(B - V)$ to T_{eff} . The distance modulus $(m - M)_V$ is taken from the several values listed in the literature. In order to obtain good average values for distance modulus, metallicity and reddening, we formed weighted averages of values taken from the literature, with the weights inversely proportional to the square of the statistical errors. It is important to note that in some cases the number of available measurements is not very large (3 or so), and that in such cases the statistical procedure was not employed. We have also calculated the reddening by comparing the $(B - V)$ vs. $(U - B)$ diagram from our data with theoretical colours from Kurucz (1993) using a least squares method. In Table 1 we show the range of metallicity data, distance modulus, reddening taken from the literature and

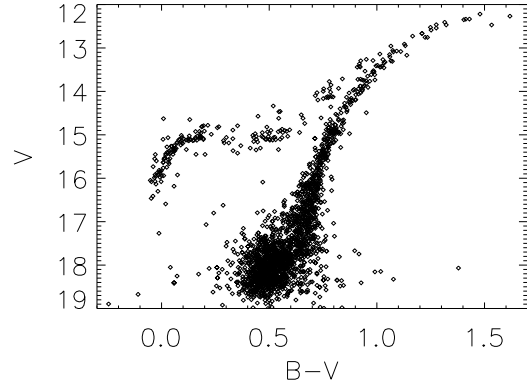


Figure 5. M5 is another globular cluster with a clear split between the RGB and the AGB. It is easy to distinguish AGB and RGB stars in the diagram.

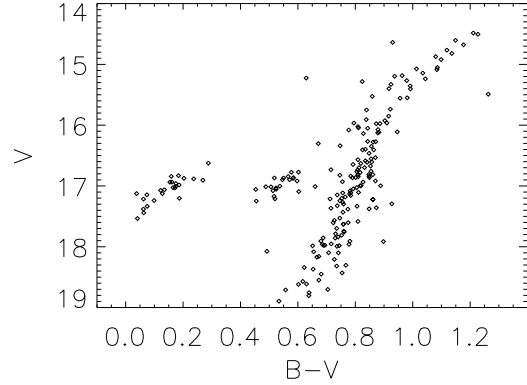


Figure 6. M72 is one of the least studied GCs in the literature. Here we present for the first time CCD data for this cluster. The HB shows a well defined RR Lyrae gap.

our adopted average values, we also include the HB colour range.

We use $Y = 0.24 \pm 0.01$ for all GCs based on standard arguments related to big bang nucleosynthesis and chemical evolution (Dorman, Vandenberg & Laskarides 1989, Pagel 1992). The bolometric correction and T_{eff} are calculated from the latest version of Kurucz stellar atmosphere models (Kurucz 1993). In Figures 2 to 6 we show the HR diagrams for the five GCs observed, corrected for reddening.

3 GLOBULAR CLUSTER REDDENING, DISTANCE MODULUS, METALLICITY, AND FIELD STAR CONTAMINATION

3.1 M68

The galactic globular cluster M68 ($l = 299.6, b = 36.0$) is a metal-poor halo globular cluster that, due to its relative openness and low reddening, is suitable for resolution of the center of the cluster. The most relevant recent studies are

	M68	M5	M72	M107
$[Fe/H]$	-2.1 to -2.0	-1.0 to -1.58	-1.5	-1.3 to -0.7
$[Fe/H](a)$	-2.0	-1.3	-1.5	-0.9
$(m - M)_V$	15.01 to 15.30	14.51 to 14.55	16.30 to 16.50	14.97 to 15.03
$(m - M)_V(a)$	15.25	14.53	16.50	14.97
$E(B - V)$	0.03 to 0.07	0.01 to 0.05	0.03 to 0.07	0.23 to 0.31
$E(B - V)(a)$	0.07	0.02	0.07	0.23
HB $(B - V)$	0.05 to 0.60	-0.05 to 0.6	0.0 to 0.6	0.85 to 1.1
	M22	M92	M3	47 Tuc
$[Fe/H]$	-1.5 to -2.0	-2.19 to -2.1	-1.69 to -1.57	-0.70 to -0.46
$[Fe/H](a)$	-1.8	-2.1	-1.6	-0.6
$(m - M)_V$	12.70 to 13.60	14.45 to 14.51	14.97 to 15.01	13.44 to 13.46
$(m - M)_V(a)$	13.50	14.45	15.01	13.46
$E(B - V)$	0.24 to 0.37	0.00 to 0.01	0.01 to 0.05	0.03 to 0.04
$E(B - V)(a)$	0.22	0.00	0.02	0.04
HB $(B - V)$	-0.25 to 0.2	-0.15 to 0.53	0.05 to 0.6	0.7 to 0.9

Table 1. The table shows the range of values for the metallicity, distance modulus and reddening taken from the literature and the adopted value in this paper. We also show the observed range in reddening-corrected $(B - V)$ colour of the HB for the set of GCs.

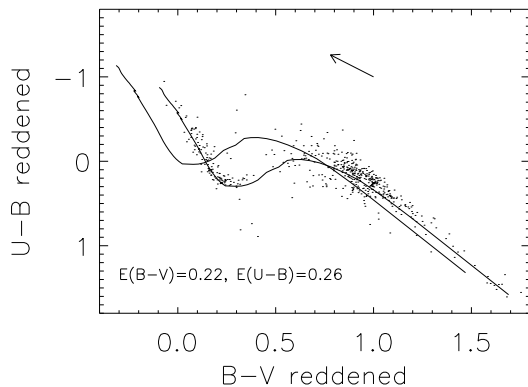


Figure 7. The two color diagram ($U - B$) vs. ($B - V$) for M22. We show the fit with an arbitrary reddening law $-E(U - B)/E(B - V)$ taken as a free parameter – to the data using Kurucz (1993) stellar atmosphere models. Also we plot the de-reddening arrow that shows the direction of the applied correction. In addition to this we have plotted the positions of Kurucz models with and without reddening correction applied.

those by Walker (1994), Alcaino et al. (1990) and McClure et al. (1987).

From the several methods available to calculate the reddening in the cluster, only one was possible using the data that we collected; the two-color diagram method in which the reddening is estimated from the offset needed to shift the observed colour-colour diagram onto the theoretical two colour diagram. A major problem is that the stellar atmosphere models used to construct the theoretical diagram do not describe the real stars equally well at all positions in the diagram. Another problem is that for the occasional cluster that lacks a well-defined HB, it is uncertain how to match the theoretical colors to the observed ones since only the RGB and whatever part of the sub-giant branch and MS that have been observed are available, and the RGB can be the part of the diagram where theoretical models are the least realistic, mainly due to problems of including enough

opacities at cool temperatures. Fortunately, for M68 the reddening is not large since the cluster is far from the galactic disk. Our fit to the observed two-color diagram with a theoretical grid of stellar atmosphere models (Kurucz 1993) gives a reddening of $E(B - V) = 0.06$. For comparison, McClure et al. (1987) and Walker (1994) found $E(B - V) = 0.07 \pm 0.01$, which is in good agreement with our value.

We adopted a value of $[Fe/H] = -2.0 \pm 0.10$.

Another source of error in the cluster color-magnitude diagrams is contamination by field stars. We estimate the severity of this effect by calculating for each cluster the number of expected field stars in the area covered by the CCD given the size of the CCD field and its galactic latitude, we have used for this purpose the model by Bachall & Soneira (1981). For M68, the number of expected field stars is around one for magnitudes brighter than 16, and so field contamination is not a serious problem.

To transform the observed HR diagram to the theoretical luminosity-effective temperature diagram, we need to know the cluster's distance modulus. From the values given in Walker (1994), Alcaino et al. (1990) and McClure et al. (1987) for M68, we have adopted an apparent distance modulus of $(m - M)_V = 15.2 \pm 0.1$.

3.2 M22

M22 is a bright globular cluster that lies in the disk of the Galaxy ($l = 9.9, b = -7.6$) and the problem of field contamination is therefore crucial. The number of field stars brighter than magnitude 16 is estimated to be about fifteen. The most recent studies of this cluster are those of Samus et al. (1995), Peterson & Cudworth (1994), Cudworth (1986) and Alcaino and Liller (1983).

Determination of the reddening for this cluster is still an open question. The published values have a large spread, ranging from $E(B - V) = 0.24$ (Crawford and Barnes 1975) to $E(B - V) = 0.37$ (Zinn 1980). Because this cluster has a well defined blue HB, we have used the two colour diagram method to find the reddening. We used two approaches. The first approach was to use a standard reddening law. The second approach was to let $E(U - B)/E(B - V)$ be a free

parameter. We found that the second approach with $E(U - B)/E(B - V) = 1.2$ produced a much better fit, giving a reddening of $E(B - V) = 0.22$ and $E(U - B) = 0.26$. We have therefore adopted these results for the reddening. In Fig. 7 we show the fit to the observed data and also the de-reddening arrow.

M22 was one of the first globular clusters for which a color-magnitude diagram was obtained (Arp & Melbourne 1959). The cluster has a low metal abundance, but the value is uncertain due to the high field star contamination. Several spectroscopic studies of M22 exist. Peterson (1980) derived metallicities ranging from $[Fe/H] = -1.62$ to -2.18 , from echelle spectra of four giant stars. Cohen (1981) carried out a detailed abundance analysis using high dispersion echelle spectra of three red giant stars and determined that they were chemically identical, with $[Fe/H] = -1.78$. Gratton (1982), also from high dispersion echelle spectra of three stars, found no indications of inhomogeneities for any element, deducing $[Fe/H] = -1.94$. Pilachowski et al. (1982) made an echelle spectral analysis of six stars near the red giant tip and derived iron abundances ranging from $[Fe/H] = -1.4$ to -1.9 . Our weighted average value for the metallicity is $[Fe/H] = -1.8$ with an uncertainty of 0.25. The spread in metallicity seems to be real and could be the reason why the RGB is intrinsically broadened in this cluster. From Fig. 3, it can be seen that the photometric errors for individual RGB stars are much smaller than the width of the RGB. We have computed the expected spread in the RGB if the metallicity ranged from $[Fe/H] = -1.5$ to $[Fe/H] = -2.0$. At a luminosity of $\log L/L_{\odot} = 2.8$, the spread would be 0.015 dex in $\log T_{\text{eff}}$, which corresponds to a spread of 0.2 in $(B - V)$. This is roughly the spread observed in the RGB of M22, and so we conclude that it is likely that the RGB in M22 is broadened by an intrinsic variation of the metal content in the cluster. The possibility of differential reddening (that would produce the same spread as the metallicity does) along the cluster cannot be completely ruled out – but it is very unlikely because stars with different metallicity in the cluster scatter all over it.

Due to the uncertainties in the reddening, an estimation of the distance modulus is difficult. We have adopted a value $(m - M)_V = 12.8 \pm 0.3$.

3.3 M72

The galactic globular cluster M72 ($l = 35.1, b = -32.7$) is not a well studied cluster. It has low metallicity and low reddening, $E(B - V) = 0.07$ (Dickens 1972). The cluster is relatively open and therefore suitable for resolving the core.

Even though the HB is not as well defined as in M22, we have, as in the previous cases, used the two colour $(B - V)$ vs. $(U - B)$ diagram to determine the reddening. We find $E(B - V) = 0.07$ using a standard reddening law, in perfect agreement with the value found by Dickens. The metallicity for the cluster, $[Fe/H] = -1.4$, has been taken from Harris & Racine (1979), and the distance modulus, $(m - M)_V = 16.3 \pm 0.1$, has been taken from Dickens (1972). Due to the characteristics of M72, the uncertainties due to reddening and metallicity are not nearly as great as for M22.

Field contamination is more severe in this case than in M68, but even so, the number of expected field stars is only five for magnitudes brighter than 17.

3.4 M5

M5 ($l = 3.9, b = 46.8$) has been the subject of many studies, most recently by Peterson (1979), Zinn (1980) and Buonanno, Corsi & Fusi Pecci (1981). It has low reddening and intermediate metallicity (Peterson 1979, Searle and Zinn 1978). From the two-colour diagram method using a standard reddening law, we determine $E(B - V) = 0.02$, in perfect agreement with the value from Buonanno et al. (1981). The value for the metallicity given by Buonanno et al. (1981) corresponds to $[Fe/H] = -1.3$, but a considerable range of values exists in the literature, from $[Fe/H] = -1.0$ (Butler 1975) to -1.58 (Zinn 1980). We have adopted $[Fe/H] = -1.2$, based on the weighted average of the literature values.

The well populated RGB is not intrinsically broad and our data allow a clear separation between the RGB and AGB stars.

3.5 M107

This cluster ($l = 3.4, b = 23.0$) has a low central concentration. The two most recent papers on M107 are Ferraro et al. (1991) and Zinn (1985). It is metal-rich, with $[Fe/H] = -0.9$ (Harris and Racine 1979). The reddening is quite uncertain, and again the RGB appears to be extremely broad, more than the intrinsic errors in the photometry.

The literature value for the reddening is $E(B - V) = 0.31$ (Zinn 1985). Using the two colour diagram method with a standard reddening law, we find $E(B - V) = 0.28$. However the alternative reddening law with $E(U - B)/E(B - V)$ a free parameter gives a better fit. We find $E(U - B)/E(B - V) = 1.13$, $E(B - V) = 0.23$ and $E(U - B) = 0.26$.

We have studied, as in M22, whether the reason for the broadened RGB could be different metallicities in the cluster. Again we have reached the conclusion that a range in metallicity of 0.5 dex could explain the RGB colour spread.

The field contamination for this cluster is not high. The number of expected stars for magnitudes brighter than 16 in V is around 10.

3.6 Other globular clusters

We have added to our sample three other GCs: M92, M3, and 47 Tuc. M92 has similar metallicity to M68 ($[Fe/H] = -2.1$ (VandenBerg 1983)). Data for the RGB in M92 is taken from the compilation in VandenBerg (1983) which relies on data from Sandage & Walker (1966) and Sandage (1969, 1970), and for the HB the colour of the reddest HB star is set by the CMDs in Sandage & Walker (1966), Buonanno et al. (1983, 1985), Rees (1992) and Montgomery & Janes (1994). The presence of HB stars on the red side of the RR Lyrae gap is in general confirmed by the values reported for $(B-R)/(B+R)$ or $B/(B+R)$, where B and R are the numbers of non-variable stars on the blue and red side of the RR Lyrae gap respectively, by Madore (1980) and Lee, Demarque & Zinn (1990) as well as the mass-distribution for the non-variable stars on the HB presented by Crocker, Rood & O'Connell (1988). 47 Tuc has been analysed in detail by Frogel, Persson and Cohen (1981) and by Dorman, VandenBerg and Laskarides (1989). We have adopted a value of $[Fe/H] = -0.6$ for this cluster. For M3, using photometric data from Buonanno et

M/M_{\odot}	Z	α	Y
0.55	0.0002	1.00	0.24
0.60	0.0005	1.25	0.28
0.65	0.001	1.50	
0.70	0.004	1.75	
0.75		2.00	
0.80			
0.85			
0.90			
0.95			
1.00			

Table 2. The table shows the stellar parameters used in the grid of stellar evolution models for the analysis of the GCs.

al (1986), we have adopted $[\text{Fe}/\text{H}] = -1.6$ (Harris & Racine 1979).

4 STELLAR EVOLUTION MODELS

The theoretical analysis of the GCs has been carried out with two theoretical tools: a classical set of stellar evolution tracks for low mass stars which we have calculated for this purpose using up-to-date input physics, and a semi-analytical stellar evolution code based on the evolution models.

Since the first grid of stellar evolution sequences for low mass stars from the main sequence to the RGT (Sweigart & Gross 1978), a large effort has been made to accurately describe the evolution of low mass stars along the RGB. Many grids of stellar evolution sequences have been published since then: VandenBerg & Bell (1985), VandenBerg (1992), Charbonnel et al. 1993, Fagotto et al. (1994). Why then the necessity for a new grid? We aimed to study the effects of variations in several parameters (mixing length ratio α , mass-loss efficiency η as parameterised in Reimers' mass-loss 'law' (Reimers 1975), total mass M , helium abundance Y and metallicity Z) on the CMD morphology. This requires a large internally consistent grid spanning the relevant parameters; such a grid does not exist in the literature. We have, therefore, calculated 130 stellar evolution sequences from the contracting Hayashi phase to the RGT. The set of parameters chosen for the grid of models is given in Table 2.

The stellar evolution code and the grid of tracks is described in detail in Jimenez & MacDonald 1995. A detailed description of the input physics can be found in Jimenez et al. (1995).

In Fig. 8 we show how the RGB is more sensitive to α than the turnoff. The effective temperature of stellar models is at least four times more sensitive to α when they are on the RGB than when they are at the main sequence turnoff. The effect of a wrong choice of α in the turnoff region is shown in Fig. 9. In the figure we show how two stars with different masses (0.75 and $0.80 M_{\odot}$, respectively) and different values of α , lie in the same position at the turnoff point. In the two tracks calculated α took values 1.25 and 1.75 respectively. From the figure we observe that the difference in $\log T_{\text{eff}}$ and in luminosity at the turnoff point between both tracks is

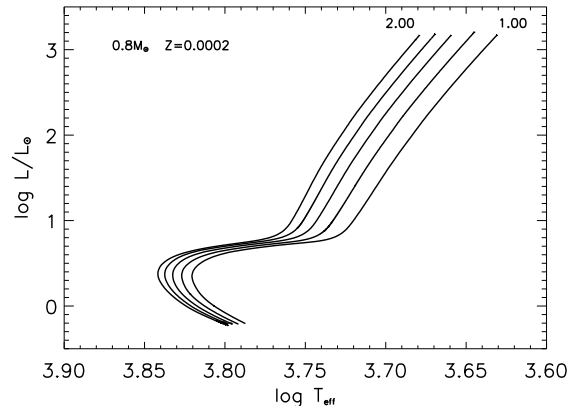


Figure 8. Effect on the RGB and main sequence turnoff of different values of α . The RGB is more sensitive to changes in α than the turnoff region.

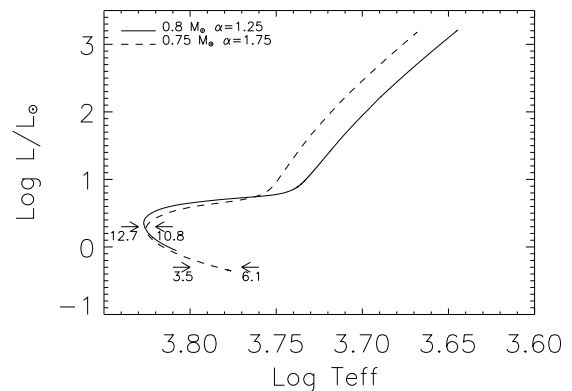


Figure 9. Two tracks with slightly different mass and α show zero sensitivity at the turnoff point. This could lead to a wrong determination of the age. The arrows show the age in Gyr. for both tracks. The arrow on the right refers to the $0.8 M_{\odot}$ track, and the arrow on the left to the $0.75 M_{\odot}$ track.

0.01 dex, and 0.2 mag, respectively – quite inside the typical observational error (see Fig. 2). On the other hand the RGBs of both clusters present a clear split of 312 K. Therefore the RGB seems to be a safer place to avoid ambiguities in the determination of α . If an isochrone is calculated from these two tracks in order to make a turnoff point fit, an error of $0.05 M_{\odot}$ could be made, which leads to an error in the age estimate of 2 Gyr.

The interesting feature of the turnoff point is that it is sensitive to the mass of the stars; therefore, in principle, it should be efficient to determine the age – a star spends 90% of its life on the main sequence – of the stars in the GC using this technique. However the location of the turnoff is not observationally well defined. This means that, in fitting an isochrone to the turnoff point, one can choose the wrong value for α and hence make an error in the mass for the stars. One of the main sources of error when using isochrone fitting is the bad definition of the turnoff point. It is not yet

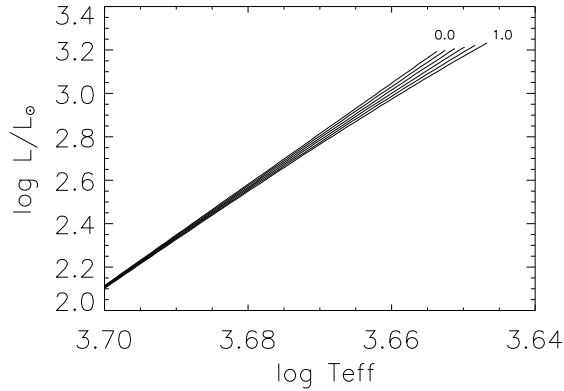


Figure 10. The effect of mass loss at the RGT. The mass loss is only important at the RGT, at the base all the tracks are similar. The η parameter has taken values from 0.0 to 1.0 in steps of 0.2. The tracks have been calculated for a model of $0.8M_{\odot}$, $\alpha = 1.4$ and $Z = 0.0002$.

clear whether the observational spread at the turnoff point is an intrinsic one, or is due only to observational errors.

The other tool that we have used is a semi-analytical stellar evolution code. A complete description of the code can be found in Jørgensen (1991), Jørgensen & Thejll (1993) and Jimenez et al. (1995). Here we will just give a brief description.

The semi-analytical method is suitable for analysis of stellar evolution on the red giant branch and on the asymptotic giant branch, with complex mass-loss scenarios included. Mass loss on the RGB is determined from Reimers' formula (Reimers 1975) with the mass loss efficiency parameter η described by a realistic distribution function based on direct observations of mass loss. This method, which we shall refer to as synthetic stellar evolution (SSE), relies on matching observational data of globular cluster red giant branch stars to theoretical results obtained by interpolation in grids of stellar evolution tracks. The key points of the synthetic method are that detailed stellar evolution models are used for the interpolation, and that the parameters in stellar evolution models, i.e., the mass-loss efficiency parameter in the Reimers formula and the mixing length parameter (α), are determined by matching the observations of the RGB as well as the HB. This assures that the physics in the SSE behaves correctly in a relative sense and is calibrated to reality which ensures the right absolute behaviour.

In brief, the SSE works in the following way:

1 The RGB part of evolutionary tracks in a given grid is fitted with analytic formulas which express the relation between L , T_{eff} , M , M_c (core-mass), Z_0 (metallicity, scaled according to $[\text{Fe}/\text{H}]$), Y (helium abundance) and α . The fitting formulas for the grid of stellar evolution models (Jimenez & MacDonald 1995) are:

$$\begin{aligned} \log L = & 4.909 + 0.032 \log Z_0 - 0.010 (\log Z_0)^2 \\ & + 2.967 \log (M_c) - 0.129 \log Z_0 \log (M_c) \\ & - 3.480 (\log (M_c))^2 \end{aligned}$$

$$\begin{aligned} \log T_{\text{eff}} = & 3.569 + 0.0640 M + 0.0126 M^2 \\ & - 0.128 \log L - 0.145 \log Z_0 + 0.0148 M \log Z_0 \\ & - 0.021 \log L \log Z_0 - 0.0250 (\log Z_0)^2 \\ & + 0.094 \log \alpha - 0.027 M \log \alpha \\ & + 0.045 \log L \log \alpha - 0.021 (\log \alpha)^2 \end{aligned}$$

$$\begin{aligned} M_c^{\text{RGT}} = & 0.456 - 0.056 M + 0.024 M^2 \\ & - 0.016 \log Z_0 + 0.002 M \log Z_0 \end{aligned}$$

where Z_0 is the solar heavy-element mass fraction scaled by $[\text{Fe}/\text{H}]$, $\log Z_0 = \log Z_{\odot} + [\text{Fe}/\text{H}]$. The goodness of fit of these equations is evaluated across the grid of points used and is always so good that errors in the observations exceed the error due to fitting.

2 The metallicity is taken from model atmosphere analyses of observed spectra in the literature. The helium abundance Y is set to 0.24 from big bang nucleosynthesis arguments (Pagel 1992).

3 With the given Z_0 and Y , it was possible to fit all the studied GCs (this paper, Jørgensen & Thejll 1993) to the analytical expressions of point 1 (or the original tracks) by use of a nominal value of the mass on the order of $0.8 M_{\odot}$ and a single value of α .

4 The detailed value of M and the average value of η are then determined by requiring agreement between the observed HB mass distribution (mean and dispersion to the red) and the modelled mass distribution calculated using numerical integration of the mass loss along the RGT. A very fast and accurate numerical computation of the evolution along the RGB is now performed by taking advantage of the expressions of point 1. The addition of mass to the core during a given time step in the integration along the RGB is determined on the basis of the instantaneous luminosity, the known energy generation rate, and the length of the time step. The mass of the core (M_c) at the end of a time step determines the new value of L according to the formulas in point 1. The total stellar mass at the end of each time step is calculated as the mass at the beginning of the time step minus the mass loss rate times the length of the time step. The evolution of the synthetic track is stopped when M_c reaches the value determined in step 1 for the He-core flash.

In a recent paper, we have demonstrated the correctness of the SSE (Jimenez et al. 1995). In particular we have shown how the SSE is accurate when calculating scenarios with mass loss and how it can be used to model the evolution along the RGB. We showed that T_{eff} and luminosity at the RGT are so relatively insensitive to the parameters of the core that the SSE reaches the same values as do the full self-consistent numerical solutions, even though for evolutionary phases with such rapid mass-loss, the full information of the mass loss does not 'reach' the core before the core-flash.

An important item when analysing GCs is the abundance of the α -elements. Many studies have found that these elements seem to be enhanced relative to Fe, compared to solar composition. Various observations have been performed in GCs in order to determine the abundance of individual elements in their RGB stars. Pilachowski, Wallerstein & Leep (1980) studied M3 and M5 and found $[\text{O}/\text{Fe}] \sim 0.3$, $[\text{Si}/\text{Fe}] \sim 0.3$. Similar results were found by Cohen (1978) in M3 and M13. Gratton, Quarta & Ortolani (1986) found the same results for all the α -elements in 47 Tuc, M4,

M5, NGC 6752 and M71. In the same vein are the results of Gratton & Ortolani (1989) for NGC 1904, NGC 3201, NGC 4590, NGC 4833, NGC 6254, NGC 6397, and NGC 6656, and Peterson, Kurucz & Carney (1990) for M92. Observations for stars in the halo also point in the direction that all the α -elements are in fact enhanced relative to solar composition (Nissen et al. 1994, Magain 1989, Wheeler, Sneden & Truran 1989). Oxygen is enhanced at about the same level as the rest of the α -elements. This is consistent with analytical models for the chemical evolution of the galaxy (Pagel & Tautvaisiene 1995).

Therefore, there is strong observational evidence that the α -elements are enhanced relative to Fe in the GCs. An important point then is: do we need new evolutionary tracks? The subject is still an open question. Two groups of researchers have put forward answers to the problem without performing detailed calculations of stellar evolution with an arbitrary abundance of α -elements.

Salaris, Chieffi and Straniero (1993) have studied the problem by comparing series of models with special combinations of enhanced α -element abundances for low mass stars. They concluded that the effect of α -element enhancements is well simulated by scaling the metallicity using the formula:

$$Z = Z_0(0.638f_\alpha + 0.362) \quad (1)$$

where Z_0 is the metallicity scaled according to iron abundance and f_α is the enhancement factor. From data in the literature a typical value for f_α is ~ 2 . A main concern with this procedure is that the effect on the opacities from the α -elements has not been ‘really’ calculated. The basic assumption by Chieffi et al. is that opacity scales as the number of α -elements. It is clear that simply scaling the Rosseland mean opacity cannot be the correct approach, and that a definitive answer will have to wait for the availability of opacities for any arbitrary composition.

The argument from the group by Vandenberg and collaborators against Chieffi et al.’s approach is that oxygen does not contribute at very low metallicity to the interior opacities. The reason for this is that at these low metallicities the opacity source is mainly due to free-free transitions of electrons from H and He. The authors argue that the rest of the α -elements do not contribute to the interior opacities, only to the boundary conditions in the stellar atmosphere. Therefore the only effect of the α -elements would be through the catalytic effect of oxygen in the CNO cycle and not in the opacities. Following this argument there is no need for arbitrary scaled opacities.

Recognising that a detailed and realistic calculation, where all the opacities for the various abundances are included, is the only way to test the effects of non-solar abundances on stellar evolutionary tracks, we decided to use both the approaches by Chieffi et al. and by Vandenberg to compute masses and ages for the set of GCs. Also we compared with simple solar scaled models i.e. $\log Z_0 = \log Z_\odot + [\text{Fe}/\text{H}]$.

It is important to know how well our parameterisation by α and η approximates reality. Obviously these two parameters represent only an empirical approximation to the real physics. They represent a parameterised macroscopic description of complex phenomena – convection and mass loss – that are happening in real stars. The point then to understand the role of α and η is to link both of them to ob-

servations. This requires that a sample of statistically useful data be gathered for them. In the case of α , a good number of stars is found at any point of the HR-diagram, but it is important to select one area where the physical conditions of the stars, in particular M , are the same. The RGB is particularly useful because the mass is strongly constrained to almost one single value along the upper part of the RGB. The η parameter has to be treated in the same way as α . In this case the mass loss is only important at the tip of the RGB. ($\dot{M} = 1.27 \times 10^{-5} \eta M^{-1} L^{1.5} T_{\text{eff}}^{-2}$).

5 HB MORPHOLOGY FROM VARIATIONS IN THE MASS LOSS EFFICIENCY

The spread of stars along the HB is mainly due to previous mass loss which varies stochastically from one star to another (Rood 1973). The range of colours where zero-age HB stars are found is a function of metallicity (the ‘‘first parameter’’) and of the range of ZAHB masses. More precisely, the ZAHB colour at given metallicity depends on both the star’s total mass and the ratio of core mass to total mass, but the core mass is essentially fixed by the physics of the helium flash and is quite insensitive to the mass and metallicity. For a given average mass loss, the average final mass is thus a decreasing function of age, which is therefore a popular candidate for the ‘‘second parameter’’ (Searle & Zinn 1978), although other candidates such as CNO abundance have also been suggested. A strong case for age as the chief (though perhaps not necessarily the only) second parameter has been made by Lee, Demarque & Zinn (1994), who find a tendency for the clusters to be younger in the outer Galactic halo. Jørgensen & Thejll (1993), using analytical fits to a variety of RGB models and following evolution along the RGB with mass loss treated by Reimers’s (1975) formula, showed that, for clusters with narrow RGB’s (the majority), star-to-star variations in initial mass, metallicity or mixing-length parameter can be ruled out as a source of the spread along the HB, leaving as likely alternatives only either variations in the Reimers efficiency parameter η (or some equivalent) or a delayed helium flash caused by differential internal rotation. The latter alternative would lead to a fuzzy distribution of stars at the RGB tip.

With our data we can analyse these propositions. Assume that there was a variation in the total mass at the flash, caused by mass loss. Looking at Fig. 10 we see that the effect on the luminosity at the helium core flash is small ~ 0.01 mag, but the effect on the temperature is quite significant $\sim 110K$. On the other hand a delayed helium core flash would not produce any effect on the effective temperature but would make stars appear above the theoretical helium core flash in a bin of ~ 0.3 mag. Considering that the evolution time in this very last bin would be the same as in the last bin before the theoretical helium core flash, we would expect the same number of stars in these two bins of the diagram. So, for a typical GC we would expect 3–4 stars. Variations in the mass loss will certainly produce variations in the morphology at the RGT. From Fig. 10, we can see what the effect on the position of the RGT is depending on the different values for η . The ‘bending’ of the RGB to lower temperatures should be, therefore, observed in HR-diagrams from GCs. This ‘bending’ should also put a constraint on the

mass distribution of stars on the HB but deficiencies with precise atmospheric boundary conditions (Alexander 1994), make this evidence qualitative rather than quantitative.

Following this strategy we looked at the previous set of observations and counted the number of stars that were expected in every bin of luminosity. Using the set of three clusters where was possible to distinguish the RGB from the AGB (M72, M68 and M5), we had a relatively good statistical sample to test the theory of a delayed helium core flash. We counted the RGB stars and compared them with the theoretical predictions. In order to calculate the number of stars expected in every bin of luminosity we used the SSE to compute the time spent there and then used the fuel consumption theorem (Renzini & Buzzoni 1986) to compute the number of stars – the integrated luminosity of the cluster was properly scaled to the area covered by the CCD. We have concluded from the set of observations that there is no GC where there appears to be an extra number of stars populating the RGB beyond the helium core flash (Fig. 11 – Fig. 14). This argument rules out, to a level of $0.01 M_{\odot}$, variations of the core mass at the flash as the cause of HB colour variations.

Therefore we are left with stochastic variations in the mass loss efficiency along the RGB as the only explanation to account for the HB morphology. An additional possible cause for the required mass loss could in theory be that the core flash is affecting the structure of the uppermost layers in such a drastic way that it could make the star lose mass at the RGT. We emphasise that the typical mass lost during the uppermost part of the RGB is about 25% of the total stellar mass. If such a large fraction of the star were to be lost to one violent effect (the He core flash), then it is very unlikely that it could happen without leaving spectral changes due to mixing of material from the core region to the surface, which are not seen in the subsequent HB star.

It is therefore meaningful to proceed to an analysis of both the RGT and the HB and link them together to deduce general properties from morphological arguments.

The SSE is the tool that we use to model the evolution along the RGB – including mass loss – and calculate the properties of the stars on the HB. In addition to this we perform some more steps to fully analyse the physical parameters on the RGB and HB of GCs. The procedure that we use in combination with the SSE to analyse the morphology of the RGB and the HB together and constrain the mass of the stars at the RGB proceeds in the following way:

- The mass on the upper part of the RGB is determined from the average mass of the HB, the average mass loss efficiency and its dispersion. Calculating the average mass and then the 2σ value of the distribution will give the range of masses along the HB. The mass difference between stars along the HB is less model dependent than the individual mass determination star by star and the average mass of the HB is better determined than the individual masses of the stars along it. The argument is twofold: the first obvious reason is that the number of stars increases and the error is statistically reduced, the second reason is that using ‘canonical’ coordinates like the ones used in Crocker, Rood and O’Connell (1988) for the zero age horizontal branch location (ZAHB) the uncertainty in the mass reduces to the uncertainty in the choice of Z but not in the location of the

stars on the ZAHB (Crocker, Rood and O’Connell 1988). Apart from this, the individual masses of the stars are much less grid dependent than the mass on the RGB. This is because M_c is very well constrained to a narrow range from theory (Jimenez et al. 1995) and therefore the luminosity as well. Also, the model grid dependence is very low. A comparison between the grid by Sweigart (1987) and the one by Dorman (1992a) gives a difference between models with identical total mass and core mass of 0.02 dex in $\log T_{\text{eff}}$, and 0.01 dex in $\log L/L_{\odot}$. This implies a difference of $0.01 M_{\odot}$ in the total mass at the ZAHB. Using a procedure similar to the one described in Crocker, Rood and O’Connell (1988) for positioning stars on the ZAHB we have determined the average mass at the HB for the set of GCs. Knowing this value and the statistical spread in mass around it, we can calculate the mass of the reddest part of the HB. The reddest part of the HB will correspond in practice to the 2σ value of the statistical distribution. This will give us the M_{RGB} , since stars with no mass-loss along the RGB will fall in the reddest part of the HB and we find that $\langle \eta \rangle - 2\sigma = 0$. Then the value of η can be computed since it has to reproduce the mean mass of the HB, constrained by the fact that $\eta = 0$ has to reproduce the 2σ value for the mass of the HB at its reddest part.

- A fit is found for the best value of α using the RGB. As we have shown the RGB is sensitive to the value of α . It is found that the same value of α fitted all the RGBs (Table 3, Jørgensen & Thejll 1993).

- The range in colour of the HB is reproduced by including mass loss along the RGB. In this way the mass of the RGB is strongly constrained since it has to reproduce the morphology of the HB.

- Now we have all the necessary parameters to model the RGB and the HB. With these data we can calculate a track and give the age at the RGT, and therefore the age of the GC itself.

In Fig. 15 we show the results of fitting tracks to the RGB with a value of $\eta = 0.0$. The distance between the abscissa of the track at the RGT and the observed stars will give an additional estimate of $\langle \eta \rangle$. As we have discussed before, mass loss does not affect the base of the RGB but it does affect the morphology of the RGT.

The importance of this procedure is that it gives a statistical map of the distribution of the mass in the HB and it sets limits to the value of η . The results for the nine clusters show that the value of η does not exceed 1.0, and that the average value is 0.4. This is in good agreement with observations on field giants (Kudritzki & Reimers 1978, Wood & Cahn 1977).

6 ANALYSIS OF THE HB IN THE GCs

Using the above method, we have analysed the RGB and HB of eight GCs. For the whole set of GCs the procedure has been the same. The first step was to compute the mean HB mass using the procedure described in Crocker, Rood and O’Connell (1988). This procedure locates the set of HB stars in a GC in a ‘canonical’ set of coordinates – in the luminosity– T_{eff} diagram – in order to reduce the model dependence of the mass determination. Once we know how the

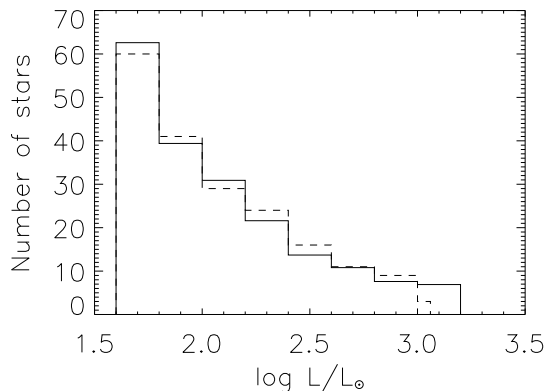


Figure 11. The histogram shows the number of stars that populate the RGB for M68. The continuous line shows the theoretical predictions and the broken line the observations. We have calculated the number of expected stars in every bin of luminosity using the formula in Renzini & Buzzoni (1986); to do it we have used the actual field of the CCD.

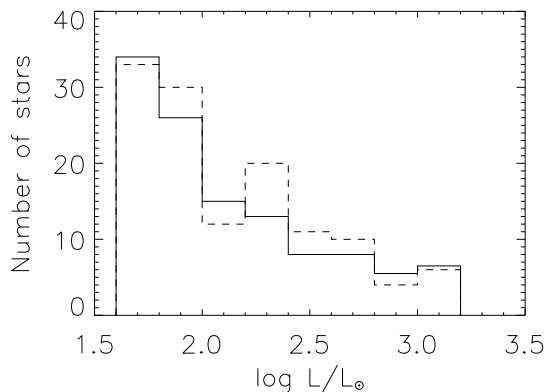


Figure 12. For the cluster M5 due to the good split between the RGB and the AGB it was easy to distinguish if there was any ‘delayed’ RGB star above the theoretical helium core flash point. None was found, in perfect agreement with the theory. The histogram confirms this result.

stars of the HB are distributed in the luminosity– T_{eff} diagram (we have used Kurucz (1993) model atmospheres), we can compute their masses using different grids of HB models. As mentioned before we have used three different approaches to account for the α -elements. For the case where only oxygen was enhanced we have used Dorman (1992b) models to compute the masses, results are presented in Table 3 column 6. In order to follow Chieffi et al.’s approach we have used Castellani, Chieffi & Pulone (1991) models with Z given by equation 1 and $f_{\alpha}=2$, the results are marked in Table 3 in column 8. The same set of models has been used for simple solar-scaled metallicities and is given in Table 3 column 7. Once the mean mass of the HB is determined and the proper value of η is applied, it is straightforward to determine the age of the GC, since now we know the mass of the RGB stars. We have used our grid of models (Jimenez & Mac-

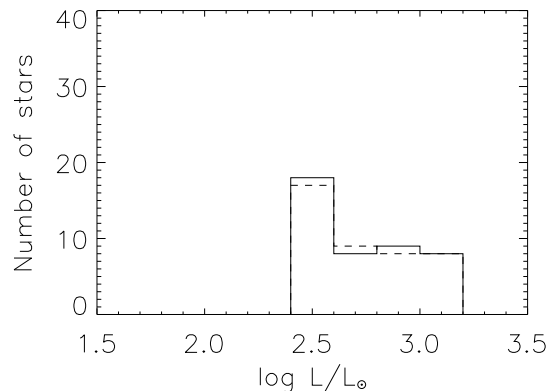


Figure 13. For M72 the agreement between the theoretical number of stars per luminosity bin and the observed ones is very good. The dashed line merges with the solid line for the last luminosity bin.

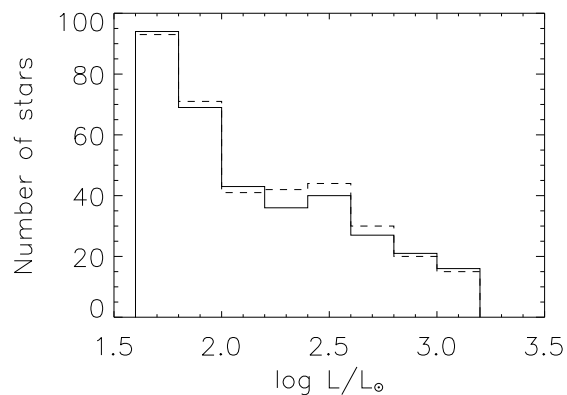
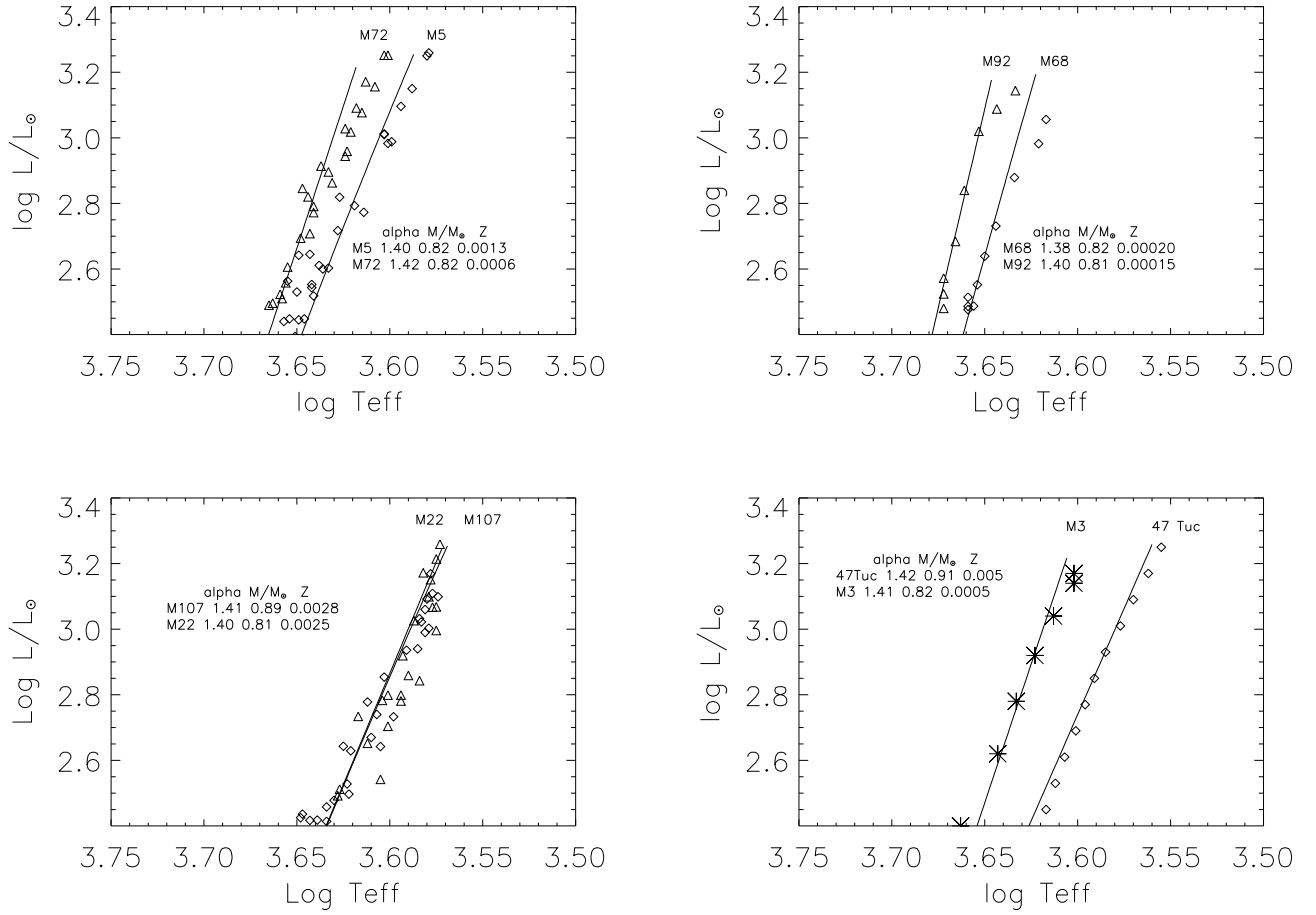


Figure 14. The figure shows the combined RGB histogram for the three GCs where it is possible to distinguish the RGB from the AGB – M68, M5 and M72. This allows to increase the statistics close to the RGT. The agreement between theory and observations is very good. There are no stars beyond the theoretical helium core flash.

Donald 1995) to compute the ages of the cases with Z_0 and Z , and the models by Bergbusch & Vandenberg (1992), to compute the ages of the O-enhanced case. The various physical parameters determined for the set of GCs are shown in Table 3. The uncertainty in all age determinations is 2 Gyr.

7 DISCUSSION

It is interesting to discuss what would be the age of the oldest GCs if all the uncertain parameters – mass determination, metallicity, helium content – are pushed in the same direction within the quoted errors. The uncertainty in Y is only ± 0.01 (see Pagel 1992), which results in an age uncertainty of 0.7 Gyr. For a cluster like M92 with a well determined Z -value of 0.0002, a change of 0.0001 will produce a change in the age of 0.1 Gyr. As we have discussed,

**Figure 15.** The RGBs of the GCs fitted in this paper

1	2	3	4	5	6	7	8	9	10	11	12	13	14
	Z_0	Z	α	$\langle \eta \rangle$	$M_{\text{HB}1}$	$M_{\text{HB}2}$	$M_{\text{HB}3}$	$M_{\text{RGB}1}$	$M_{\text{RGB}2}$	$M_{\text{RGB}3}$	$t1$	$t2$	$t3$
					O-enh	Z_0	Z	O-enh	Z_0	Z	O-enh	Z_0	Z
M92	0.00015	0.0002	1.40	0.4	0.67	0.71	0.71	0.77	0.81	0.81	12.9	13.2	13.2
M68	0.0002	0.0003	1.38	0.4	0.68	0.73	0.73	0.78	0.82	0.82	12.6	12.6	12.7
M22	0.0004	0.0007	1.40	0.4	0.64	0.69	0.69	0.78	0.81	0.81	13.5	13.5	13.7
M3	0.0005	0.0008	1.41	0.4	0.65	0.72	0.72	0.78	0.82	0.82	13.2	13.0	13.5
M72	0.0006	0.0009	1.42	0.4	0.65	0.71	0.71	0.78	0.82	0.82	12.7	13.0	13.5
M5	0.0013	0.0021	1.40	0.4	0.65	0.70	0.70	0.79	0.82	0.82	12.9	13.0	13.8
M107	0.0028	0.0046	1.41	0.4	0.72	0.77	0.77	0.85	0.89	0.89	12.3	12.0	13.2
47 Tuc	0.005	0.008	1.42	0.4	0.74	0.78	0.78	0.88	0.91	0.91	11.6	11.5	13.0

Table 3. The table shows the physical parameters calculated for the GCs. Z_0 is the solar scaled metallicity according to $[\text{Fe}/\text{H}]$. Z represents the metallicity in the GC according to Salaris, Chieffi and Straniero (1993), but with $f_{\alpha} = 2$. α is the mixing length parameter fitted from the RGB. $\langle \eta \rangle$ has been calculated from the value to reproduce both the point in the HB with $\eta = 0$ and the the mean average HB mass, also from the ‘bending’ of the RGT – except for M68 and M92, where the determination from the ‘bending’ was not possible and only the first method was applied. Column 6 gives the mean HB mass calculated from the models by Dorman (1992b) with O/Fe enhanced. The following two columns represent the computation of the mean HB mass from the models by Castellani, Chieffi and Pulone (1991), using effective metallicities Z_0 and Z respectively. The next three columns show the corresponding values for the mass at the RGB; 1 corresponds to models with only [O/Fe] enhanced, 2 models with metallicity Z_0 and 3 models with metallicity Z .

an uncertainty in the mass of $0.03 M_{\odot}$ will produce an error on the age estimate of 2 Gyr. As first shown by Stringfellow et al. (1983), gravitational settling of helium and the concomitant displacement of the major nuclear fuel, hydrogen, from the stellar core has the effect of shortening main sequence lifetimes. Recent studies by Proffitt & Vandenberg (1991) and Chaboyer et al. (1992) find an age reduction of about 1 Gyr. It is important to note that although this process has a major effect on the position of the main sequence turnoff in the HR diagram, the effect on the position of the RGB is negligible. This means that our method is basically unaffected by the process of helium settling, except that, if helium settling is important and not washed out by mixing processes, our ages from standard evolutionary tracks would have to be reduced by 0.5–1.0 Gyr. In the most extreme case, combination of these effects gives a maximum age reduction of 3.8 Gyr, so that for M92 we would obtain an age as low as 9.7 Gyr. Therefore GCs ages as low as 10 Gyr cannot be totally ruled out, but it is important to emphasise that this is the extreme lower limit, and that unless stellar evolution theory is completely wrong or some hidden physics is playing an important role, ages of GCs cannot be lower than 10 Gyr.

It is important to notice that variations needed in M_c alone to produce the observed spread in colour in the HB are about $0.1 M_{\odot}$, but would also produce a ‘vertical’ spread in luminosity of 0.5 mag – according to the models by Dorman (1992a) and Castellani, Chieffi & Pulone (1991). This is obviously much bigger than the real spread observed in GCs’ HBs (Fig. 2–6). This is another argument to rule out the theory of a delayed core flash, and also rules out the possibility that random variations in the core mass due to the helium core flash take place between the RGT and the HB rapid evolution phase.

Those GCs that present a thick RGB show also a spread in luminosity on the HB. Using the models by Dorman (1992a) and Castellani, Chieffi & Pulone (1991) we see that a spread of 0.5 dex in [Fe/H] would produce a spread in the luminosity of the HB of 0.3 mag. It is nice to see that this is roughly the spread observed in the HB of M22 and M107. On the other hand clusters with a very well defined and thin RGB like M68 show an admirably thin HB. It is tentatively concluded that the spread in luminosity on the HB could be due to different metallicities, but two clusters give too little statistics to draw a definitive conclusion. A large number of clusters has to be observed.

In the calculation of the age of the globular clusters the main ingredient and delicate point is the mass determination. An error in the mass of $0.05 M_{\odot}$ will lead to an uncertainty in the age of 3 Gyr. Therefore it is very important to know the accuracy of our mass determination. From the different grids of models published we found a spread of $0.01 M_{\odot}$. The procedure to calculate the average mass of the HB is very consistent in itself and the internal accuracy of the procedure is $0.005 M_{\odot}$, which is smaller than likely systematic effects related to uncertainties in the physics of the horizontal branch (semi-convection etc.) and the effects of non-standard chemical composition. An error of $\pm 0.03 M_{\odot}$ will give an uncertainty of ± 2 Gyr. (Jimenez & MacDonald 1995), which we believe to be a reasonable estimate of our uncertainties. One advantage of our method is that it is virtually independent of the distance modulus. In comparison,

	$(m - M)_v$ fit to RGT	$(m - M)_v$ prev.
M68	15.20	15.25
M22	13.60	13.50
M72	16.30	16.50
M5	14.51	14.53
M107	15.03	14.97
M3	15.00	15.01
M92	14.50	14.45
47 Tuc	13.46	13.46

Table 4. The third column shows the values of the distance modulus for the set of GCs observed in this study. The distance moduli have been calculated from the fit to the upper part of the RGB up to the RGT. This method gives a general uncertainty of 0.05 mag – see explanation in the text. The column to the right represents the values adopted from the literature.

the age determination from isochrone fitting has a typical uncertainty of 3–4 Gyr. as we have shown from a bad choice of the mixing length and a bad definition of the turnoff itself, as well as uncertainties in the distance.

From the previous photometric data for the RGBs of the set of GCs, it was clear that the non-existence of ‘delayed’ RGB stars gives an obvious method to calculate the distance modulus of the cluster. Since the luminosity of the RGT does not change much in the mass range $0.8\text{--}0.9 M_{\odot} - 0.04$ mag (Jimenez & MacDonald 1995) – and is almost independent of metallicity, a fit to the observed histogram at the last leg of the RGB would give a very accurate determination of the distance modulus. We have used this procedure to make a consistency test of our method and recalculate the distance modulus. In Table 4 we present the results of our fitting procedure to the RGT with theoretical models. As we pointed out before the intrinsic error in this determination is 0.04 mag.

Assuming the masses we have derived to be correct, an important question is how much of the missing physics could affect the age determination in our method. Two scenarios that could seriously affect the method are related to helium diffusion and a more realistic treatment of the opacity problem for non-scaled solar abundances. The problem of the opacities for the α -elements has been discussed in the text and there is much neglected in this field. A necessity for arbitrary composition stellar evolution sequences is obvious.

The helium diffusion problem has been studied by Proffitt & Vandenberg (1991) and Chaboyer et al. (1992). They find that it will lead to an age reduction of about 1 Gyr. The reason for this age reduction comes from the fact that less H is available for burning due to He sinking into the core. It is important to notice that the position of the RGB and the HB are almost unaffected by this process – while the position of the turn-off point obviously is. This means that our method is basically affected by the process of helium diffusion only to the extent that this affects the evolutionary lifetime along the MS. As a result of this, if helium diffusion is proven to be important, we would have to cut by 0.5–1.0 Gyr. the ages calculated from our standard evolutionary tracks.

The ‘second parameter’ problem refers to clusters with the same (intermediate) metallicity but different HB morphologies. The most common resource is to explain it by

age differences among the clusters. From our study we have concluded that the origin of the HB morphology is due to a spread of the mass loss efficiency along the RGB, but centred around a well defined value of $\eta = 0.4$. This may or may not be the case for the ‘second-parameter’ clusters. However, our results show that, if indeed these clusters are younger, then their initial mass of the stars on the RGB will be slightly greater, and then a similar mass loss rate superposed on an unchanged core mass will lead to thicker envelopes and a redder HB. Therefore, a consistency result of the method claims that since the average η is the same for all the clusters, the mass at the RGB has to be different in order to produce different HB morphologies. This would imply that age difference is, in fact, the explanation for the ‘second parameter’ problem. We therefore confirm previous solutions to this problem (Lee, Demarque & Zinn 1994). All studies that include the HB get a good agreement on the age, e.g. 47 Tuc (Dorman, VandenBerg & Laskarides 1989).

Finally, we make some comments on the comparison of our results with those of the more conventional method based on turn-off luminosity, itself depending on the magnitude difference ΔV between the HB and the turnoff. The HB is calibrated either on the basis of HB models, such as we have also used (e.g. Chaboyer, Sarajedini & Demarque 1992; Salaris, Chieffi & Straniero 1993), or from luminosities of RR Lyrae stars based on Baade-Wesselink pulsation analysis (Carney, Storm & Jones 1992), the same adjusted to fit extragalactic cepheids (Walker 1992), or analysis of the Oosterhoff period-shift effect (Sandage 1993). The Walker and Sandage scales give the greatest distances and hence the shortest ages (the range of about 0.3^m between HB calibrations gives a range of 25 per cent in age, while uncertainty in ΔV itself gives a further 10 per cent or so and more in some cases; cf. comments by Carney et al. on M68, to which they assign an age of 21.3 Gyr (taking $[\alpha/H] = [O/H] = 0.3$), the same as for M92, although the formal result from ΔV is only 16.4 Gyr). Bergbusch & VandenBerg (1992), using oxygen-enhanced models, suggest an age of 14 Gyr for M92, very similar to our values; this requires adoption of a relatively large distance modulus, $(m-M)_V = 14.7$, compared to Carney et al.’s adopted modulus of 14.3; these moduli essentially straddle the range between extreme (semi-empirical) calibrations of RR Lyrae luminosities, while our adopted modulus for M92 is 14.5. The remaining discrepancy between our value and that of Bergbusch & VandenBerg, when their modulus is replaced by ours, is about 3Gyr, a gap that is readily bridged by differing model assumptions.

This last claim is supported by a comparison with the work of Chaboyer, Sarajedini & Demarque (1992), who use an α -enhanced chemical composition that seems to us very realistic ($[O/Fe] = [\alpha/Fe] = 0.4$; cf. Pagel & Tautvaisiene 1995), and that of Salaris, Chieffi & Straniero (1993) who use a somewhat more α -enhanced mixture. A comparison of the clusters that we have in common is given in Table 5.

It transpires from the table that our ages are not in serious disagreement with those deduced from turn-off magnitudes, bearing in mind differences in adopted distance, and the large discrepancies that occasionally occur even when the same distance is adopted. Chaboyer (1995) quotes an average age of 14.2 Gyr for the lower-metallicity clusters, using the Walker distance scale, and a minimum possible age of 11 Gyr. There is thus no evidence for serious system-

atic errors in our method, and we consider that the fit to the RGB luminosity function that we have made provides a more robust method of distance determination than the RR Lyrae method. Our results also show that internal rotation and diffusion effects have little influence on the HB core masses.

8 CONCLUSIONS

In this paper we have presented clues for two important questions in stellar evolution and cosmology: the spread in colour of the HB and the age of the oldest known stars in the universe. Using very accurate photometry that we have obtained on five globular clusters we were able to distinguish for three of them the RGB from the AGB with no ambiguity.

With these data we studied the possible scenarios to produce the spread in colour on the horizontal branch. The theory of a delayed helium core flash would produce an extra number of stars above the theoretical helium flash point. We have seen that this is not happening. Also, variations in the core mass would produce a vertical spread in the HB that is not observed, except in cases where there is also a spread in the RGB – due to metallicity variations – and these metallicity variations could account for the vertical spread. The only scenario left to explain the spread in colour along the HB is that variations in the mass loss along the RGB produce a different ratio of total mass to core mass. As a consequence of this we have concluded that the explanation for the ‘second parameter’ problem relies on age differences among the clusters that present this effect – different masses at the RGB. Even though a different value for $\langle \eta \rangle$ among these clusters could produce the same result, the question would be, why should these clusters have a different value of $\langle \eta \rangle$?

Once the nature of the HB has been explained we have used the morphology of the RGT to constrain the amount of mass that is lost at this stage of stellar evolution. Using this and the morphology of the HB we have been able to put strong constraints on the mass of the RGB stars. We have calculated ages for the GCs in the sample and found that the oldest clusters have an age of 13.5 Gyr. This estimate of the age is in better agreement with current cosmological models, especially an open universe with $H_0 \approx 80 \text{ km s}^{-1} \text{ Mpc}^{-1}$ (Freedman et al 1994, Pierce et al 1994).

Now we are in the position to answer all the questions that we formulated in the introduction:

- i) The HB morphology is well explained by differential variations in the mass loss efficiency along the RGB among the stars. The distribution of the HB mass is gaussian. In the case of η a value of $\langle \eta \rangle = 0.4$ is found for the set of GCs studied.
- ii) Since mass loss is the cause of the HB morphology, the properties of the stars at the RGT can be linked with those at the HB. This gives a powerful method to constrain the mass of the RGB.
- iii) The mean mass of the HB and the 2σ value of the HB mass distribution have been used to determine the value of η and the mass at the RGB
- iv) The HB morphology is explained as variations in η , but with a central value of $\langle \eta \rangle = 0.4$ which is the same for all the clusters. The ‘second parameter’ problem is explained as

	(m-M) _V Chaboyer	Age (Gyr)	(m-M) _V Salaris	Age (Gyr)	(m-M) _V This work	Age (Gyr)
M92	14.6	17.0	14.5	18.4	14.5	13.2
M68	15.2	12.9	15.15	14.2	15.2	12.7
M3	15.1	14.2	15.0	15.6	15.0	13.5
M5	14.5	13.3	14.4	15.0	14.5	13.8
M107	15.0	14.0	14.85	15.9	15.0	13.2
47 Tuc	13.35	14.0	13.2	18.0	13.5	13.0

Table 5. The table shows the different age estimates for different assumptions of the distance modulus. Also, we show the comparison of conventional main sequence turn-off fitting with our method.

a mass difference among clusters with identical metallicity, and therefore as an age difference among them.

v) The age for the oldest GCs was (13.5 ± 2) Gyr. A 1σ uncertainty in each of the parameters of mass and helium content combined with the effects of helium diffusion gives a lower limit for the age of the oldest clusters of 9.7 Gyr.

ACKNOWLEDGEMENTS

RJ acknowledges support from the EU under the Human and Capital Mobility grant 920014. PT acknowledges support from the Carlsberg foundation. We thank C. Flynn, H.R. Johnson, B. Jones, B. Madore, J. Ostriker, A. Renzini and D. Seckel for a careful reading of the manuscript and helpful discussions and comments.

REFERENCES

Alcaino, G., Liller, W., 1983 AJ, 88, 1330
Alcaino, G., Liller, W., Alvarado, F., Wenderoth, E. 1990, AJ, 93, 114
Alexander D., 1994, *Private communication*
Arp, H.C., Melbourne, W.G., 1959, AJ, 64, 28
Bahcall J.N., Soneira R.M., 1981, ApJS, 47, 357
Bencivenni, D., Castellani, V., Tornambé, A., Weiss, A., 1989 ApJS, 71, 109
Bergbusch, P.A. & Vandenberg, D.A. 1992 ApJS, 81, 163
Bergeron P., Saffer R.A., Liebert J. 1992, ApJ 394, 228
Böhm-Vitense, E., 1958. Z. Astrophys., 46, 108
Buonanno, R., Buscema, G., Corsi, C.E., Iannicola, G., Smriglio, F., 1983, AAS 53, 1
Buonanno, R., Buzzoni, A., Corsi, C.E., Fusi Pecci, F., & Sandage, A.R., 1986, Mem. Soc. Astr. Ital., 57, 391
Buonanno, R., Corsi, C.E., Fusi Pecci, F., 1981, MNRAS, 196, 435
Buonanno, R., Corsi, C.E., Fusi Pecci, F., 1985, AA 145, 97
Butler, D. 1975, ApJ, 200, 68
Carney, B.W., Storm, J., Jones, R.V. 1992, ApJ, 386, 663
Castellani, V., Chieffi, A., Pulone L. 1991, ApJS, 76, 911
Chaboyer, B., 1995, ApJ, 444, L9
Chaboyer B., Deliyannis C.P., Demarque P., Pinsonneault M.H., Sarajedini A. 1991, 1992, 388, 372
Chaboyer, B., Demarque, P., Pinsonneault, M.H. 1992, ApJ, 395, 515
Chaboyer, B., Sarajedini, A., Demarque, P., 1992 ApJ, 394, 515
Charbonnel C., Meynet G., Maeder A., Schaller G., Schaerer D., 1993, A&AS 101, 415
Cohen, J.G., 1978, ApJ, 223, 487
Cohen, J.G., 1981, ApJ, 247, 869
Crawford, D.L., Barnes, J.V., 1975, PASP, 87, 65
Crocker D.A., Rood R.T., O'Connell R.W., 1988, ApJ 332, 236

Cudworth, K.M., 1986, 92, 348
Dickens, R.J., 1972, MNRAS, 157, 281
Dorman, B., 1992a, ApJS 80, 701
Dorman, B., 1992b, ApJS 81, 221
Dorman, B., Vandenberg, D.A., Laskarides, P.G., 1989, 343, 750
Fagotto F., Bressan A., Bertelli G., Chiosi C, 1994 A&AS, 105, 29
Ferraro, F.R., Clementini, G., Fusi Pecci, F., Buonanno, R., 1991, MNRAS, 252, 357
Fowler, W.A., Caughlan, G.R., Zimmerman, B.A. 1975, ARA&A, 13, 69
Freedman W.L., Madore B.F., Mould J.R., Hill R., Ferrarese L., Kennicutt R., Saha A., Stetson P.B., Graham J.A., Ford H., Hoessel J.G., Huchra J., Hughes S.M., Illingworth G.D., 1994, Nature, 371, 757
Frogel J.A., Persson S.E., Cohen J.G., 1981, ApJ, 246, 842
Gratton, R.G., 1982, A&A, 115, 336
Gratton R.G., Quarta, M.L., Ortolani, S. 1986, A&A, 169, 208
Gratton, R.G., Ortolani, S., 1989, A&A, 1989, 211, 41
Harris, W.E. 1975, ApJS, 29, 397
Harris, W.E., Racine, R., 1979, ARA&A, 17, 241
Harris, M.J., Fowler, W.A., Caughlan, G.R., Zimmerman, B.A. 1983, ARA&A, 21, 165
Iben, I., Renzini, A., 1984, Phys. Rep. 105, 329
Jimenez R., 1995, PhD Thesis
Jimenez, R., Jørgensen, U., Thejll, P., MacDonald, J., 1995a, MNRAS, 275, 1245.
Jimenez, R., MacDonald, J., 1995, MNRAS in press.
Jørgensen U.G., 1991, A&A, 246, 118
Jørgensen U.G., Thejll P., 1993, A&A, 272, 255
Kudritzki R.P., Reimers D., 1978, A&A 70, 227
Kurucz, R. 1993, CDROM 13
Landolt, A.U., 1992, AJ, 104, 340
Lee Y., Demarque P., Zinn R., 1990, ApJ, 350, 155
Lee Y., Demarque P., Zinn R., 1994, ApJ, 423, 248
Madore, B. F. 1980, in *Globular Clusters*, D. Hanes, & B. Madore (eds.), CUP, p. 21
Magain, P. 1989, A&A, 209, 211
McClure, R., Vandenberg, D.A., Bell, R.A., Hesser J.E., Stetson P.B., 1987, AJ, 93, 1144
Montgomery, K.A., Janes, K.A., 1994, in *Hot Stars in the Galactic Halo*, S.J. Adelman, A.R. Upgren and C.J. Adelman (eds.), CUP, p. 136
Nissen P.E., Gustafsson B., Edvardsson B., Gilmore G. 1994, A&A, 285, 440
Pagel B.E.J., 1992, In: F. Sanchez, M. Collados, R. Rebolo (eds), *Observational and physical Cosmology*, Cambridge University Press, p. 117.
Pagel B.E.J., Tautvaisiene, G. 1995, MNRAS 276, 505
Peterson, R.C., 1979, in J.E. Hesser (ed.), IAU Symp. 185: *Star Clusters*, Reidel, Dordrecht, p. 461
Peterson, R.C., 1980, ApJ, 237, 87
Peterson, R.C., Kurucz, R.L., Carney, B.W. 1990, ApJ, 350, 173
Peterson, R.C., Cudworth, K.M., 1994, ApJ, 420, 612

- Pierce M.J., Welch D.L., McClure R.D., van den Bergh S., Racine R., Stetson P.B., 1994, *Nature*, 371, 385
- Pilachowski, C.A., Wallerstein, G., Leep, E.M. 1980, *ApJ*, 236, 508
- Pilachowski, C.A., Leep, E.M., Wallerstein, G., Peterson, R.C., 1982, *ApJ*, 263, 187
- Proffitt C.R., VandenBerg D.A. 1991, *ApJS*, 473, 514
- Rees,, F.R., Jr., 1992, *AJ* 103, 1573
- Reimers D., 1975, *Mem. Soc. Roy. Sci. Liege* 8, 369
- Renzini A., Buzzoni A. 1986, *Spectral evolution of galaxies: Proceedings of the Fourth Workshop*, Erice, Italy. Dordrecht: D. Reidel Publishing Co.
- Rood, R.T. 1973, *ApJ*, 184, 815
- Salaris, M., Chieffi A., Straniero O., 1993, *ApJ*, 414,580
- Sandage, A., 1969, *ApJ* 157, 515
- Sandage, A., 1970, *ApJ* 162, 841
- Sandage, A., 1982, *ApJ*, 252, 553.
- Sandage, A., 1993, *AJ*, 106, 719
- Sandage, A., & Walker, M.F. 1966, *ApJ*, 143, 313
- Samus, N., Kravtsov, V., Pavlov, M., Alcaïno, G., Liller, W, 1995, *A&AS*, 109, 487
- Searle, L., Zinn, R., 1978, *ApJ*, 225, 357
- Stetson, P.B., 1987, *PASP*, 99, 191
- Stetson, P.B., 1992, User's Manual for DAOPHOT II
- Stringfellow G.S., Bodenheimer P., Noerdlinger P.D., Arigo R.J., 1983, *ApJ*, 264, 228
- Sweigart A. V. 1987, *ApJS* 65, 95
- Sweigart A., Gross P.G. 1978, *ApJS*, 36, 405
- VandenBerg, D.A., 1983, *ApJS*, 51, 29.
- VandenBerg, D.A., 1988, In: J.E. Grindlay and A.G. Davis Philip (ed.), *The Harlow-Shapley Symposium on Globular Cluster Systems in Galaxies*.
- VandenBerg, D.A., 1992, *ApJ*, 391, 685
- VandenBerg, D.A., Bell, R.A., 1985, *ApJS*, 58, 561
- VandenBerg, D.A., Bolte, M., Stetson, P.B., 1990, *AJ*, 100, 445
- Walker, A., 1992, *ApJ*, 390, 81
- Walker, A., 1994, *AJ*, 108, 555
- Wheeler J.C., Sneden C., Truran J.W. 1989, *ARAA*, 27, 279
- Wood P.R., Cahn J.H., 1977, *ApJ* 211, 499
- Zinn, R., 1980, *ApJS*, 42, 19
- Zinn, R., 1985, *ApJ*, 293, 424